

## CRYSTALLIZATION, PHASE TRANSITIONS AND THERMAL STABILITY OF LADDER-TYPE $(M_2Cu_2O_3)_m(CuO_2)_n$ CUPRATES

V. Maltsev\*, N. I. Leonyuk

Department of Crystallography and Crystal Chemistry, Geological Faculty,  
Moscow State University, Moscow 119992, Russia

A new family of  $(M_2Cu_2O_3)_m(CuO_2)_n$  ( $M=Ca, Sr, Bi, rare\ earth\ elements$ ) single crystals was grown. The structural analysis has shown that these crystals differ from the other phases of this group by unstable oxygen content in the fragment of the crystal lattice containing the ribbons of Cu-O squares. The differential thermal and thermogravimetry analysis of two crystalline  $(M_2Cu_2O_3)_m(CuO_2)_n$  samples,  $(Ca_{6.7}Sr_{7.0}Bi_{0.3})Cu_{23.0}O_x$  and  $(Ca_{6.9}Sr_{6.8}Bi_{0.3})Cu_{23.3}O_x$ , were carried out for the first time on this type of cuprates.

(Received July 10, 2003; accepted August 21, 2003)

*Keywords:* Crystal growth, Low dimensional structures, Phase transitions, Superconducting materials, Cuprates

### 1. Introduction

For the first time, high- $T_c$  superconductivity at 80-85 K and normal/ambient pressure was observed in the spin ladder single crystals  $(M_2Cu_2O_3)_m(CuO_2)_n$  ( $M = Ca, S, Bi, Y, rare\ earth\ element$  (RE) and  $m/n = 1/1$  or  $5/7$ ) grown from fluxed melts [1]. Also, nearly simultaneously, the authors of ref. [2] have observed superconductivity in the ceramic sample  $Sr_{0.4}Ca_{13.6}Cu_{24}O_{41.84}$  under hydrostatic pressure of 3 to 4.5 Gpa with a relatively low critical temperature 10 K. Then, it was found [3] that the superconductivity manifests itself at normal pressures only in the crystals in the region of a low-temperature  $\alpha$ -modification of incommensurate-type  $(M_2Cu_2O_3)_m(CuO_2)_n$  phases ( $\alpha$ -IP) [4], i.e., at the maximum temperatures not higher than 960 °C. The interpretation of this observation should be related to the difference between low-temperature  $\alpha$ -IP and high-temperature ( $\beta$ -IP) modifications which has not been investigated up to now. In superconducting samples, Ca-amount should exceed Sr, and the Ca/Sr ratio, as a main condition for manifestation of superconductivity, was directly confirmed by a single crystal X-ray analysis of superconducting (SC) and non-superconducting (NSC)  $(M_2Cu_2O_3)_m(CuO_2)_n$  crystals [5]. Another condition, which could be related to the manifestation of superconductivity, is the  $m/n$ -value of  $(M_2Cu_2O_3)_m(CuO_2)_n$  phase. However, a commensurate version of the structure for the same sample can be described by various  $m/n$ -values [6,7]. Therefore, a correlation between this parameter and superconducting properties is difficult to be done. In this work, recent experimental data on the growth and properties of  $(M_2Cu_2O_3)_m(CuO_2)_n$  single crystals of various composition and structure are presented, and their thermal stability as well as phase transitions are discussed.

### 2. Experimental

Single crystals of  $(M_2Cu_2O_3)_m(CuO_2)_n$ -type phases were grown from the high temperature solutions based on the  $Bi_2CuO_4$  and  $BaCuO_2$  fluxes, i.e.  $1.5RE_2O_3-22(Ba,Sr,Ca)O-75CuO$  and

Corresponding author: maltsev@geol.msu.ru

$2\text{Bi}_2\text{O}_3\text{-}3.2\text{CaO(YO}_{1.5}\text{)-}2.8\text{SrO-}4\text{CuO}$  initial fluxed melt compositions, by well known cooling, decanting [8] and "melted band" [3] methods. All experiments were carried out under the conditions which differ by the maximum ( $T_{max}$ ) and minimum ( $T_{min}$ ) temperatures using  $\text{Al}_2\text{O}_3$  and  $\text{ZrO}_2$  crucibles. In the case of the "melted band" technique, a negative temperature gradient in the furnace was distributed in such a way that the melting occurs only at the superheated crucible walls (Fig. 1a). The solvent from the load at the top and in the middle is melted and flows down to the hot zone at the bottom of the crucible. The incommensurate-type single crystals grow in the relatively cold zone. Therefore, the most important conditions for success are the followings: (1) the rod in the middle and the crust at the top are not destroyed, (2) the drops of the  $\text{Bi}_2\text{Sr}_2\text{CaCu}_2\text{O}_8$  (2201) phase from the vaporising melt are deposited on the relatively cold surface of the incommensurate-type crystals (Fig. 1b).

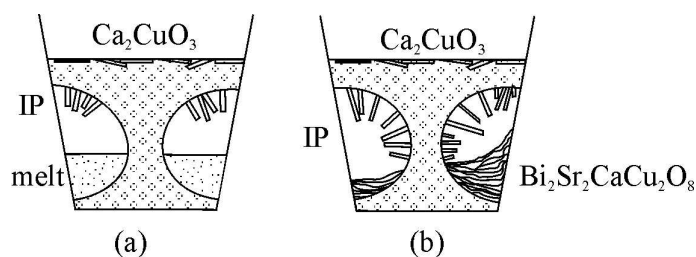


Fig. 1. The scheme of the crystal growth by the "melted band" method.

The X-ray powder diffraction patterns were obtained making use of a diffractometer INEL XRG 3000 (Capillary-Debye Scherrer Geometry) with  $\text{Cu } K\alpha$ -radiation. The data were interpreted using the program EVA-Solid Solutions, v.5.0, rev. 2 (Bruker Analytical X-ray System) and PC PDF Data Base (1998, JCPDS, International Center for Diffraction Data). Chemical composition of the samples were measured by means of a scanning electron microscope Jeol JSM-5800LV (20 kV).

The differential thermal and thermogravimetry analysis (DTA and TGA respectively) of two crystalline  $(\text{M}_2\text{Cu}_2\text{O}_3)_m(\text{CuO}_2)_n$  samples with total weight  $\sim 60$  mg in each run were performed at air ambient. The temperature was increased up to  $1050^\circ\text{C}$  at  $2^\circ\text{C/h}$  and decreased with the same rate.

### 3. Results and discussion

#### 3.1. Crystallization and crystallo-chemical features

Table 1 shows some of the results obtained in more than 30 experimental runs on single crystal growth in the temperature regime corresponding to the existence of  $\alpha$ -IP phase. All crystals of the runs 800, 1031, 1098 and 1317 were SC with the ratio  $\text{Ca/Sr} \geq 1$  and characterized by  $m/n=7/10$  according to the X-ray structural analysis. In this case, using a decanting method,  $T_{max}$  and  $T_{min}$  were corresponded to the temperature of the phase transition  $\text{SrCuO}_2$  -  $\beta$ -IP ( $980^\circ\text{C}$ ), and the  $\alpha$ -IP -  $\beta$ -IP equilibrium ( $960^\circ\text{C}$ ), respectively. If  $T_{max}$  was in the region of  $1010\text{-}1015^\circ\text{C}$ , i.e., in the field of the phase  $\text{SrCuO}_2$  stability, but  $T_{min}$  was kept in the range of  $\alpha$ -IP phase, NSC RE-cuprate crystals were grown by cooling technique at a rate of  $1.5\text{-}4.0^\circ\text{C/h}$  (run numbers 1284, 1285, 1286, 1289). Similar results were also obtained in the runs 1292 (cooling method at the rate of  $0.8^\circ\text{C/h}$ ,  $T_{max}=1040^\circ\text{C}$ ,  $T_{min}=300^\circ\text{C}$ ), 1298 (decanting technique,  $T_{max}$  was in the region of the phase  $\text{SrCuO}_2$  stability, and  $T_{min}=960^\circ\text{C}$ ), and 1369 (decanting method,  $T_{max}$  and  $T_{min}$  were in the region of the  $\beta$ -IP phase).

The Sr-concentration was always higher than Ca in the crystals obtained at high  $T_{max}$ -values. In this case the  $m/n$ -ratios were  $7/10$  or  $5/7$ . The  $m/n=5/7$ -values correlated with the presence of yttrium in the crystal. At lowering temperature of  $4^\circ\text{C/h}$  (1289), the ratio  $m/n$  was equal to  $13/18$  (according to the X-ray structural analysis), whereas for the sample 1292 obtained in regime with a low cooling rate,

the  $m/n$ -value was corresponded to 1/1. When regime was used at high cooling rates, the single crystals with Nd and Sm (runs 1284 and 1286) were platelets with  $m/n=13/18$ . The Nd-containing crystal without Ba (number 1285) obtained at low cooling rate (1.5°C/h) was needle-like with  $m/n=7/10$ . Pr-containing crystals were always plate-like.

Table 1. Characteristics of grown crystals.

Run #	Composition	Lattice constants, Å			Space group	T <sub>c</sub> , K
		a	b	c		
1284	(Y <sub>2.2</sub> Nd <sub>5.5</sub> Sr <sub>9.7</sub> Ba <sub>0.6</sub> )Cu <sub>31.0</sub> O <sub>53</sub>	11.296(1)	12.8850(9)	3.9686(3)	Fmmm	NSC
1285	(Y <sub>1.3</sub> Nd <sub>3.7</sub> Sr <sub>2.5</sub> Ca <sub>6.5</sub> )(Cu <sub>23.2</sub> Ca <sub>0.4</sub> Sr <sub>0.4</sub> )O <sub>41</sub>	11.299(6)	12.515(2)	27.541(6)	Abmm	NSC
1286	(Y <sub>1.3</sub> Sm <sub>3.2</sub> Sr <sub>3.7</sub> Ca <sub>9.8</sub> )Cu <sub>30.5</sub> O <sub>53</sub>	11.312(2)	12.946(2)	3.9510(6)	Fmmm	NSC
1289	(Y <sub>2.2</sub> Pr <sub>5.2</sub> Sr <sub>10.0</sub> Ba <sub>0.6</sub> )Cu <sub>30.7</sub> O <sub>53</sub>	11.3183(8)	12.967(2)	3.9616(6)	Fmmm	NSC
1292	Y <sub>0.12</sub> Pr <sub>0.29</sub> Sr <sub>0.56</sub> Ba <sub>0.03</sub> Cu <sub>1.91</sub> O <sub>3</sub>	11.331(4)	12.972(7)	3.9672(8)	Fmmm	NSC
1298	(Sr <sub>5.96</sub> Y <sub>0.53</sub> Ca <sub>3.12</sub> Bi <sub>0.12</sub> )Cu <sub>16.55</sub> Al <sub>0.26</sub> O <sub>28.45</sub>	11.346(3)	12.996(3)	19.585(9)	F222	NSC
800	(Sr <sub>4.42</sub> Ca <sub>4.86</sub> Bi <sub>0.05</sub> )Cu <sub>17</sub> O <sub>29</sub>	11.349(7)	12.896(5)	19.49(3)	F222	82
1031	Sr <sub>0.49</sub> Ca <sub>0.48</sub> Bi <sub>0.03</sub> Cu <sub>1.69</sub> O <sub>2.99</sub>	11.361(4)	12.906(7)	3.9067(8)	Fmmm	85
1098	(Sr <sub>4.02</sub> Ca <sub>5.84</sub> Bi <sub>0.14</sub> )Cu <sub>15.84</sub> O <sub>29</sub>	11.346(2)	12.809(3)	19.52(1)	F222	82
1317	(Sr <sub>3.56</sub> Y <sub>0.10</sub> Ca <sub>6.02</sub> Bi <sub>0.28</sub> )Cu <sub>16.45</sub> O <sub>28.63</sub>	11.319(2)	12.763(2)	19.49(1)	F222	80
1369	Sr <sub>0.14</sub> Ca <sub>0.69</sub> Bi <sub>0.16</sub> Cu <sub>1.71</sub> O <sub>2.91</sub>	11.393(5)	13.042(5)	3.9137(9)	Fmmm	NSC

The structure of ladder-type incommensurate phases is similar to a well-known 123-type (YBa<sub>2</sub>Cu<sub>3</sub>O<sub>7</sub>) structure. In both layer-type structures two Cu-O motifs of different dimensionality present. Two conditions for a manifestation of superconductivity can be formulated. The first condition is related to the occurrence of high carrier concentration, which manifest itself by an increase of the formal Cu-valence in one-dimensional (1D) motif. The second condition is related to an efficient transfer of free carriers into the 2D motif and can be characterized by the distance between Cu-atoms located in the chain/ribbon and plane.

The estimation of the role of these conditions is more complicated in the case of incommensurate-type phases than in 123-type compounds because of a large unit cell, incommensurate modulation of lattice parameters and wide spectrum of isomorphous substitutions. It should be noted that in the *M*-site of  $(M_2Cu_2O_3)_m(CuO_2)_n$ -type crystals a large variety of elements were found: Ca, Sr, Ba, Bi, large RE elements of Ce-group and small RE elements of Y-group. Different coordination by oxygen atoms is typical of these cations: 10-apical polyhedron for Ba, twisted cube for Sr, cube for Ca and probably for Y, 8-apical polyhedron for large RE, octahedron for Bi, etc. The changes in the structure of cation polyhedra lead primarily to the deformations of the ribbon fragment. The presence of *M*-cations of various valences influences the formal valence of Cu.

Thus, a comparison of the structures in the scale of interatomic distances is possible for only compounds of a similar composition. Such investigations were made in [3] by studying two, SC and NSC,  $(M_2Cu_2O_3)_m(CuO_2)_n$  crystals.

### 3.2. Differential thermal and thermogravimetric analysis

The differential thermal and thermogravimetric analysis of two crystalline  $(M_2Cu_2O_3)_m(CuO_2)_n$  samples, (Ca<sub>6.7</sub>Sr<sub>7.0</sub>Bi<sub>0.3</sub>)Cu<sub>23.0</sub>O<sub>x</sub> (1) and (Ca<sub>6.9</sub>Sr<sub>6.8</sub>Bi<sub>0.3</sub>)Cu<sub>23.3</sub>O<sub>x</sub> (2), were carried out for the first time on this type phases. Both these samples were superconducting before and after experiment and they were grown at different regimes by the "melted band" method at temperatures about 900 °C and 830 °C.

During the heating of the first sample, the thermal effects are quite clearly seen at 970 and 980°C which can be related to transitions  $\alpha$ -IP -  $\beta$ -IP and  $\beta$ -IP - (Sr,Ca)CuO<sub>2</sub>, respectively (Fig. 2a). The effect at 1030 °C coincides with the melting point of SrCuO<sub>2</sub>. At cooling, the first effect is observed at 1010 °C due to crystallization of (Sr,Ca)CuO<sub>2</sub>. The transition (Sr,Ca)CuO<sub>2</sub> -  $\beta$ -IP manifests itself relatively weakly at 985 °C. A strong effect at 960 °C corresponds probably to the transition  $\beta$ -IP -  $\alpha$ -IP.

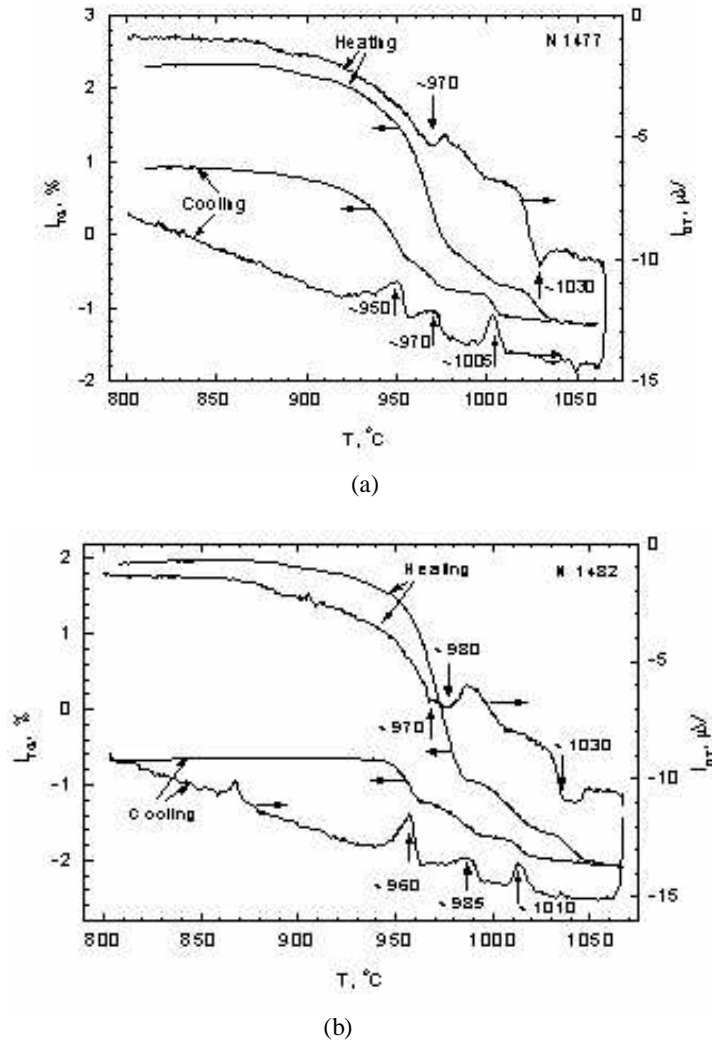


Fig. 2. DTA/TGA data for samples  $(Ca_{6.7}Sr_{7.0}Bi_{0.3})Cu_{23.0}O_x$  (a) and  $(Ca_{6.9}Sr_{6.8}Bi_{0.3})Cu_{23.3}O_x$  (b).

The change of the growth regime for the second sample has led to an absence of the effect due to transition  $\alpha$ -IP -  $\beta$ -IP in the DTA curve at heating (Fig. 2b). The other two effects assigned to transition  $\beta$ -IP - (Sr,Ca)CuO<sub>2</sub> and melting of (Sr,Ca)CuO<sub>2</sub> are quite clearly seen. The reduction of crystallization temperature for (Sr,Ca)CuO<sub>2</sub> as well as due to transitions (Sr,Ca)CuO<sub>2</sub> -  $\beta$ -IP and  $\beta$ -IP -  $\alpha$ -IP can be also caused by the presence of bismuth which favors a decrease of crystallization temperature and contributes to ordering of the structure in the ribbon layer.

Two additional effects should be noticed in the DTA curves for the sample 1. A weak effect is seen at 900 °C at heating and quite strong effect is resolved in the region of 870 °C at cooling. Taking into account that the X-ray powder diffraction analysis of the sample with a similar mass shown the presence of about 4% of the phases Bi-2201 and Bi-2212 ( $Bi_2Sr_2CaCu_2O_8$ ), the effects mentioned above can be explained by the contribution of these phases. At re-melting, the phase 2201 probably

transfers completely to 2212. It is interesting to note that these effects are absent in the second sample. This fact puts in doubt a prescription of the Bi-rich phase separated at the decomposition of solid solution to the phase Bi-2212.

The effects on TGA curves are related to the weight loss at melting and to the weight increase at crystallization. As a whole, these effects correspond to those in DTA curves and can be related to the loss and absorption of oxygen in the disordered Cu-O ribbon.

#### 4. Conclusions

The crystallization conditions of the  $(M_2Cu_2O_3)_m(CuO_2)_n$ -type phases were analyzed and the single crystals with the structure close to the unstable phase  $\beta$ -IP were grown. The structural analysis has shown that this phase differs from the other phases of this group by unstable oxygen content in the fragment of the crystal lattice containing the ribbons of Cu-O squares.

The differential thermal and thermogravimetry analysis of two crystalline  $(M_2Cu_2O_3)_m(CuO_2)_n$  samples,  $(Ca_{6.7}Sr_{7.0}Bi_{0.3})Cu_{23.0}O_x$  (1) and  $(Ca_{6.9}Sr_{6.8}Bi_{0.3})Cu_{23.3}O_x$  (2), were carried out for the first time on this type phases.

The obtained results allow one to reveal the regularities in the phase formation of  $(M_2Cu_2O_3)_m(CuO_2)_n$  compounds and to specify the conditions for the growth of SC single crystals of incommensurate-type phases.

#### Acknowledgements

The research described in this publication was supported, in part, by the grant of Russian President for young scientists MK-1430.2003.05.

#### References

- [1] L. Leonyuk, G. J. Babonas, A. Vasilev, R. Szymczak, A. Reza, V. Maltsev, L. Ponomarenko, Czech J. Phys. **46**, Suppl. S3, 1457 (1996).
- [2] M. Uehara, T. Nagata, J. Akimitsu, H. Takahashi, N. Mori, K. Kinoshita, J. Phys. Soc. Jpn **65**, 2764 (1996).
- [3] V. Maltsev, L. Leonyuk, G.-J. Babonas, R. Szymczak, A. Reza, J. Cryst. Growth **211**, 501 (2000).
- [4] B. V. Slobodin, A. A. Fotiev, A. S. Kosmyrin, G. E. Shter, N. K. Garkushin, V. L. Balashov, A. S. Trunin, Sverkhprovodimost: FKhT **3**, 523 (1990) (in Russian).
- [5] L. Shvanskaya, L. Leonyuk, E. Sokolova, V. Maltsev, Z. Kristallogr. **215**, 368 (2000).
- [6] A. F. Jensen, F. K. Larsen, B. B. Iversen, V. Petricek, T. Schultz, Y. Gao, Acta Cryst. **B53**, 113 (1997).
- [7] L. Leonyuk, G.-J. Babonas, V. Chernyshov, V. Rybakov, V. Maltsev, M. Baran, Acta Cryst. **A56**, 149 (2000).
- [8] V. Maltsev, L. Leonyuk, G.-J. Babonas, A. Vetkin, A. Reza, J. Cryst. Growth **198/199**, 626 (1999).